

## COMMUNICATION



# Adsorption of two gas molecules at a single metal site in a metal–organic framework†

Cite this: *Chem. Commun.*, 2016, 52, 8251

Received 23rd March 2016,  
Accepted 3rd June 2016

DOI: 10.1039/c6cc02494g

www.rsc.org/chemcomm

Tomče Runčevski,<sup>ab</sup> Matthew T. Kapelewski,<sup>ab</sup> Rodolfo M. Torres-Gavosto,<sup>ab</sup>  
Jacob D. Tarver,<sup>cd</sup> Craig M. Brown<sup>ce</sup> and Jeffrey R. Long<sup>\*abf</sup>

**One strategy to markedly increase the gas storage capacity of metal–organic frameworks is to introduce coordinatively-unsaturated metal centers capable of binding multiple gas molecules. Herein, we provide an initial demonstration that a single metal site within a framework can support the terminal coordination of two gas molecules—specifically hydrogen, methane, or carbon dioxide.**

Metal–organic frameworks have been explored extensively for possible applications in the storage of hydrogen,<sup>1</sup> methane,<sup>2</sup> and other gases<sup>3</sup> and possess the inherent advantage that lower pressures and higher temperatures can be utilized than currently feasible with common compression or cryogenic storage. Notably, the geometry and size of the framework pores, the types of internal surfaces, and the nature of the resident binding sites all heavily influence gas adsorption properties. In particular, an important strategy to increase storage capacities and meet the U.S. Department of Energy passenger vehicle system targets for storing H<sub>2</sub> at 40 g L<sup>-1</sup> and 5.5 wt% at pressures up to 100 bar and ambient temperatures<sup>4</sup> is to increase the density of strong binding sites within the pores of a given framework.<sup>5</sup>

Typically, the strongest binding sites for gas molecules are coordinatively-unsaturated metal centers,<sup>1c,e,2a–c,5–7</sup> which can present binding enthalpies as high as –21.6 kJ mol<sup>-1</sup> for methane

in Ni<sub>2</sub>(dobdc) (dobdc<sup>4-</sup> = 2,5-dioxido-1,4-benzene-dicarboxylate)<sup>2e</sup> and –13.7 kJ mol<sup>-1</sup> for hydrogen in Ni<sub>2</sub>(*m*-dobdc) (*m*-dobdc<sup>4-</sup> = 4,6-dioxido-1,3-benzenedicarboxylate).<sup>6g</sup> Importantly, although these materials also boast a high density of open metal coordination sites, each metal is only capable of adsorbing a single gas molecule, thus limiting the storage capacity. To date, the terminal coordination of more than one gas molecule at a single metal site has not been rigorously demonstrated within a metal–organic framework. While the design of new frameworks with a high concentration of low-coordinate metal centers presents an important and ongoing research challenge, certain existing structure types may present an opportunity for demonstrating the viability of this strategy.

It was recently shown that the thiolated analogue of the dobdc<sup>4-</sup> linker, 2,5-disulfido-1,4-benzenedicarboxylate (dsbdc<sup>4-</sup>), combines with Mn<sup>2+</sup> to form the DMF-solvated framework Mn<sub>2</sub>(dsbdc)(DMF)<sub>2</sub>·0.2DMF.<sup>8</sup> In this structure, two distinct octahedral metal centers alternate down helical chains running along the crystallographic *c*-axis, one with six ligating atoms arising from dsbdc<sup>4-</sup> linkers and the other with just four. Importantly, two terminal DMF molecules bound in a *cis* configuration complete the coordination sphere of the latter type of Mn<sup>2+</sup> site. Herein, we demonstrate a means of fully activating this material while retaining a high degree of crystallinity. As probed by *in situ* powder diffraction measurements, the resulting four-coordinate metal centers can indeed each adsorb two gas molecules.

After synthesis according to the literature procedure,<sup>8</sup> exchange of the DMF in Mn<sub>2</sub>(dsbdc)(DMF)<sub>2</sub>·0.2DMF with methanol and subsequent heating at 423 K under dynamic vacuum yielded the fully desolvated material, Mn<sub>2</sub>(dsbdc). This compound exhibits a Langmuir surface area of 1610 m<sup>2</sup> g<sup>-1</sup> based upon N<sub>2</sub> adsorption at 77 K (see the ESI†); purity and complete activation were confirmed by infrared spectroscopy and elemental analysis (see the ESI†). Often, large single crystals of metal–organic frameworks do not survive activation conditions and instead form a micro-crystalline powder. Thus, considering that the activation of Mn<sub>2</sub>(dsbdc)(DMF)<sub>2</sub>·0.2DMF could alter the original framework topology, we sought to verify the structure of activated Mn<sub>2</sub>(dsbdc) *ab initio* from synchrotron X-ray powder diffraction data.

<sup>a</sup> Department of Chemistry, University of California Berkeley, Berkeley, California 94720, USA. E-mail: jrlong@berkeley.edu

<sup>b</sup> Materials Sciences Division, Lawrence Berkeley National Laboratory, Berkeley, California 94720, USA

<sup>c</sup> Center for Neutron Research, National Institute of Standards and Technology, Gaithersburg, Maryland 20899, USA

<sup>d</sup> National Renewable Energy Laboratory, 15013 Denver West Parkway, Golden, Colorado 80401, USA

<sup>e</sup> Department of Chemical and Biomolecular Engineering, University of Delaware, Newark, Delaware 19716, USA

<sup>f</sup> Department of Chemical and Biomolecular Engineering, University of California Berkeley, Berkeley, California 94720, USA

† Electronic supplementary information (ESI) available: Gas adsorption, Langmuir fitting, elemental analysis, infrared spectroscopy, X-ray powder diffraction, neutron powder diffraction, inelastic neutron scattering spectroscopy. See DOI: 10.1039/c6cc02494g

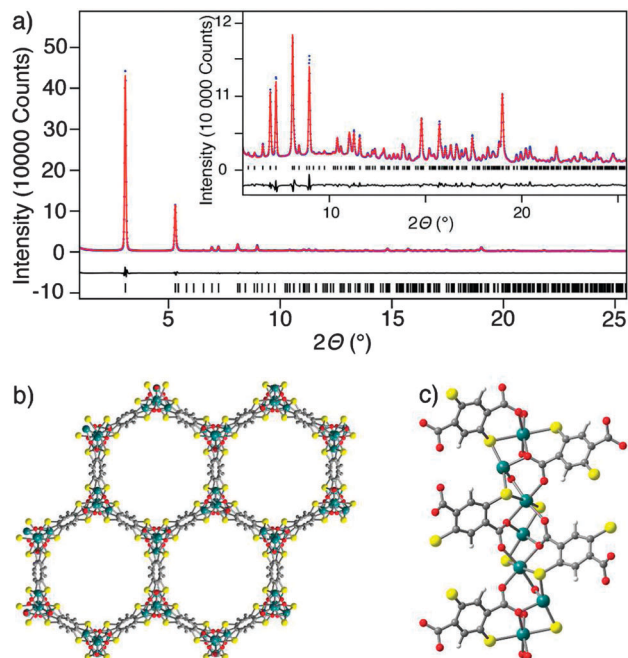


**Fig. 1** (a) Rietveld plot for the crystal structure of  $\text{Mn}_2(\text{dsbdc})$ . The scattered X-ray intensity is represented by blue dots, the best fit with a red line, the difference curve with a gray line, and the Bragg positions with vertical bars. The high-angle portion of the pattern is enlarged in the inset for clarity. (b) Crystal structure of  $\text{Mn}_2(\text{dsbdc})$  showing the one-dimensional hexagonal pores along the crystallographic  $c$ -axis. (c) A portion of a single helix of alternating six-coordinate and four-coordinate metal nodes, with blue-green, yellow, red, gray, and white spheres representing Mn, S, O, C, and H atoms, respectively.

The corresponding Rietveld plot is presented in Fig. 1a (experimental details can be found in the ESI†).

Crystallographic analysis confirmed the complete desolvation of the framework and formation of  $\text{Mn}_2(\text{dsbdc})$  with a crystal packing isostructural to the solvated framework. The structure consists of infinite  $\text{Mn}^{2+}$  helices running along the crystallographic  $c$ -axis, and these chains are connected by  $\text{dsbdc}^{4-}$  linkers to form a honeycomb structure (Fig. 1b) containing one-dimensional channels with a van der Waals diameter of  $\sim 16$  Å. In the asymmetric unit, there are two crystallographically independent  $\text{Mn}^{2+}$  ions bridged by the thiophenoxide and carboxylate groups of the anionic  $\text{dsbdc}^{4-}$  linkers (Fig. 1c). One of the  $\text{Mn}^{2+}$  ions is six-coordinate and adopts an octahedral geometry with four oxygen atoms at the equatorial positions (Mn–O bond lengths of 2.19(2) and 2.27(2) Å) and two axial sulfur atoms (Mn–S bond lengths of 2.575(7) Å). The second  $\text{Mn}^{2+}$  ion is four-coordinate, exhibiting a see-saw geometry, with the two opposing coordination sites occupied by sulfur atoms (Mn–S bond lengths of 2.405(7) Å) and the two intervening sites occupied by oxygen atoms (Mn–O bond lengths of 2.07(1) Å). Relative to the corresponding octahedral site in the DMF-solvated crystal structure, this  $\text{Mn}^{2+}$  ion sits slightly displaced toward the remaining *cis* equatorial oxygen atoms, resulting in a relatively bent S–Mn–S angle of 159.3(2)° (compared to the S–Mn–S angle of 176.0° in  $\text{Mn}_2(\text{dsbdc})(\text{DMF})_2 \cdot 0.2\text{DMF}$ ).<sup>8</sup> Regardless, its geometry appears to leave ample open space in which two gas molecules could approach the positive charge density of the  $\text{Mn}^{2+}$  ion.

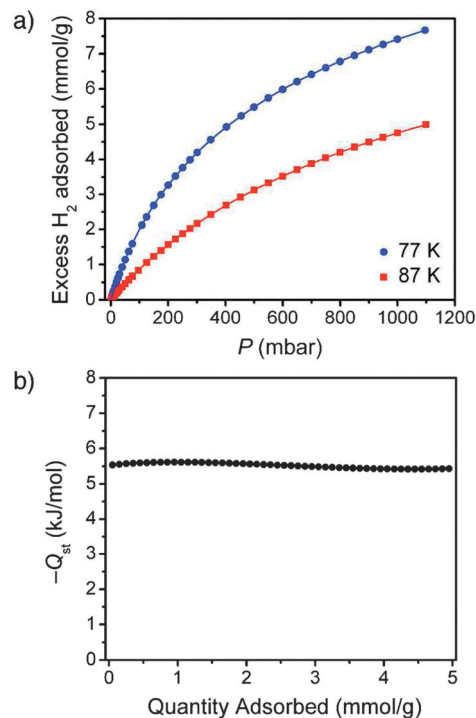


**Fig. 2** (a) Experimental  $\text{H}_2$  isotherms for  $\text{Mn}_2(\text{dsbdc})$  at 77 K (blue circles) and 87 K (red squares). Blue and red lines represent dual-site Langmuir isotherm fits. (b) Isothermic heat of  $\text{H}_2$  adsorption in  $\text{Mn}_2(\text{dsbdc})$ , as calculated using the Clausius–Clapeyron relation.

To evaluate the  $\text{H}_2$  adsorption properties of  $\text{Mn}_2(\text{dsbdc})$ , isotherms were measured at 77 and 87 K (Fig. 2a). The isotherms do not rise steeply compared to a number of other metal–organic frameworks possessing exposed metal cation sites, suggesting that the  $\text{Mn}^{2+}$  ions within this structure do not have an unusually strong affinity for  $\text{H}_2$ .<sup>1,4</sup> Each isotherm was independently fit using a dual-site Langmuir model. By interpolating data points from the resulting fits at constant loadings, the isosteric heat of  $\text{H}_2$  adsorption in  $\text{Mn}_2(\text{dsbdc})$  could be determined for the various loadings (Fig. 2b). Indeed, as expected from the isotherm shapes, only a very modest initial binding enthalpy of  $-5.6$   $\text{kJ mol}^{-1}$  is observed, indicating that the  $\text{Mn}^{2+}$  ions in the  $\text{S}_2\text{O}_2$  see-saw coordination geometry of  $\text{Mn}_2(\text{dsbdc})$  only weakly polarize the  $\text{H}_2$  molecules. We note that there is precedent for weaker interactions with  $\text{Mn}^{2+}$  as compared with other metals. For comparison, the isosteric heat of  $\text{H}_2$  adsorption in  $\text{Mn}_2(\text{dobdc})$  is  $-8.8$   $\text{kJ mol}^{-1}$ ,<sup>6g</sup> which represents the weakest binding enthalpy of the  $\text{M}_2(\text{dobdc})$  series, while that within  $\text{Ni}_2(m\text{-dobdc})$  is  $-12.3$   $\text{kJ mol}^{-1}$ .<sup>6g</sup> The ability of the large  $\text{Mn}^{2+}$  to only weakly polarize  $\text{H}_2$  coupled with the lack of space available around the  $\text{Mn}^{2+}$  center due to the larger radius of sulfido donor atoms relative to oxido donor atoms lead to this relatively weak binding enthalpy.

Despite this low adsorption enthalpy, the anticipated binding of two hydrogen molecules at a single metal site is readily apparent from neutron powder diffraction experiments carried out on  $\text{Mn}_2(\text{dsbdc})$  for  $\text{D}_2$  loadings of 0.7 and 1.4 per four-coordinate metal ion (Rietveld plots are presented in Fig. S5 and S6 in the ESI†). Fig. 3 presents a portion of the crystal structure surrounding

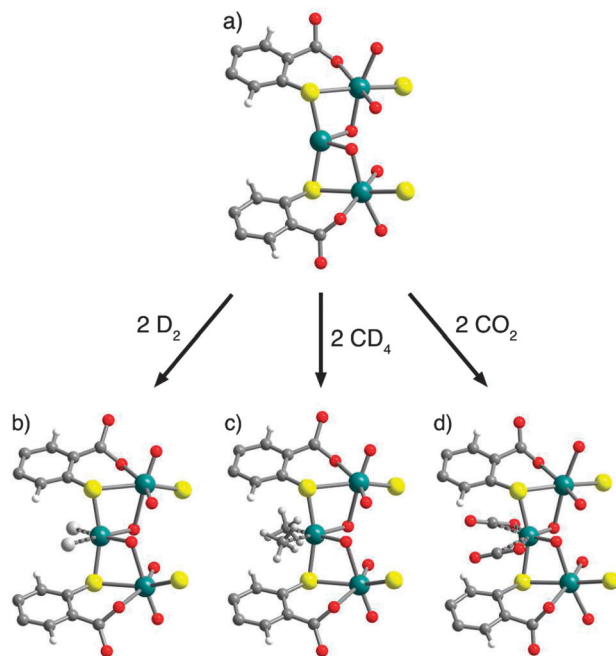


**Fig. 3** Top: A portion of the crystal structure of  $\text{Mn}_2(\text{dsbdc})$  presented around the four-coordinate  $\text{Mn}^{2+}$  center in (a) activated, (b) 0.7  $\text{D}_2$  dosed, (c) 0.4  $\text{CD}_4$  dosed, and (d) 0.13  $\text{CO}_2$  dosed samples (per four-coordinate metal ion). Blue-green, yellow, red, gray, and small white spheres represent Mn, S, O, C, and D or H atoms, respectively. Large white spheres in (b) represent the centroids of  $\text{D}_2$  molecules. Selected interatomic distances and angles: (a)  $\text{Mn}-\text{O} = 2.07(1) \text{ \AA}$ ;  $\text{Mn}-\text{S} = 2.405(7) \text{ \AA}$ ;  $\angle \text{S}-\text{Mn}-\text{S} = 159.3(2)^\circ$ ; (b)  $\text{Mn}-\text{D}_2 = 3.40(4) \text{ \AA}$ ;  $\text{Mn}-\text{O} = 2.19(5) \text{ \AA}$ ;  $\text{Mn}-\text{S} = 2.34(6) \text{ \AA}$ ;  $\angle \text{S}-\text{Mn}-\text{S} = 164(4)^\circ$ ; (c)  $\text{Mn}\cdots\text{C}(\text{CD}_4) = 3.66(1) \text{ \AA}$ ;  $\text{Mn}-\text{D}(\text{CD}_4) = 2.72(3) \text{ \AA}$ ; (d)  $\text{Mn}-\text{O}(\text{CO}_2) = 3.55(10) \text{ \AA}$ ;  $\text{Mn}\cdots\text{C}(\text{CO}_2) = 3.52(10) \text{ \AA}$ . For refinement of (c) and (d) the framework parameters were kept fixed.

the four-coordinate metal center before (Fig. 3a) and after (Fig. 3b) dosing with 0.7 equivalents of  $\text{D}_2$ . The interaction of two  $\text{D}_2$  molecules with a single  $\text{Mn}^{2+}$  ion is clearly observed for this loading. The  $\text{Mn}-\text{D}_2$  separations of 3.40(4) and 3.07(3)  $\text{ \AA}$  for  $\text{D}_2$  loadings of 0.7 and 1.4, respectively, again indicate relatively weak interactions between the gas molecules and the metal ion. For comparison, the very strongly polarizing five-coordinate  $\text{Co}^{2+}$  ions in  $\text{Co}_2(m\text{-dobdc})$  result in a  $\text{Co}-\text{D}_2$  separation of just 2.23(5)  $\text{ \AA}$ .<sup>6e</sup> Although association with the metal center represents the primary binding site, there is also a secondary (lower-occupancy) binding site that could be identified within the structure of  $\text{Mn}_2(\text{dsbdc})\cdot 0.7\text{D}_2$ , as well as a tertiary binding site in  $\text{Mn}_2(\text{dsbdc})\cdot 1.4\text{D}_2$ . The  $\text{Mn}^{2+}-\text{H}_2$  association is further supported by the results of inelastic neutron scattering spectroscopy (INS) experiments performed upon dosing  $\text{Mn}_2(\text{dsbdc})$  with  $\text{H}_2$  (see the ESI† for details). The INS data indicate an association of the  $\text{H}_2$  with the  $\text{Mn}^{2+}$  through a splitting and shifting of the quantum rotational levels beyond that experienced by  $\text{H}_2$  in the bulk or weakly physisorbed  $\text{H}_2$ .

Gratifyingly, we were also able to solve  $\text{CD}_4$ - and  $\text{CO}_2$ -dosed structures of  $\text{Mn}_2(\text{dsbdc})$  using neutron and X-ray powder diffraction, respectively (experimental details and Rietveld plots are given in the ESI†). This demonstrated that a variety of different gases can interact with the exposed four-coordinate

metal sites within the framework. Fig. 3c presents a portion of the crystal structure showing binding of two  $\text{CD}_4$  molecules at a single metal center, with corresponding  $\text{Mn}-\text{D}$  and  $\text{Mn}\cdots\text{C}$  distances of 2.72(3) and 3.40(1)  $\text{ \AA}$ , respectively. Fig. 3d presents the same part of the structure after adsorption of two  $\text{CO}_2$  molecules, with  $\text{Mn}-\text{O}$  and  $\text{Mn}-\text{C}$  distances of 3.55(10) and 3.52(10)  $\text{ \AA}$ , respectively. We note that the separations between the metal center and the adsorbed gas molecules are somewhat longer than observed within frameworks featuring more polarizing metal cation sites.<sup>6b,d,f-h,7</sup>

In conclusion, we have demonstrated that coordinatively unsaturated  $\text{Mn}^{2+}$  centers in the metal-organic framework  $\text{Mn}_2(\text{dsbdc})$  can adsorb two terminally bound gas molecules simultaneously. While the binding strength of  $\text{H}_2$  in this framework is modest compared to materials such as  $\text{Ni}_2(m\text{-dobdc})$ ,<sup>6g</sup> this result represents an important proof of concept that we hope will inform the further design of materials with drastically improved gas storage properties. For example, replacing the four-coordinate  $\text{Mn}^{2+}$  ions within the structure of  $\text{Mn}_2(\text{dsbdc})$  with larger metal cations, such as  $\text{Ca}^{2+}$ , could further expose the metal ion charge density, leading to stronger binding of  $\text{H}_2$  and perhaps even coordination of three  $\text{H}_2$  molecules.

This research was supported through the Department of Energy, Office of Energy Efficiency and Renewable Energy, Fuel Cell Technologies Office (under grant DE-AC02-05CH11231). X-ray diffraction measurements were performed at Beamline 17-BM, Advanced Photon Source, Argonne National Laboratory, Proposal ID: 46636. M. T. K. and R. M. T.-G. gratefully acknowledge support through the NSF Graduate Research Fellowship Program. J. D. T. gratefully acknowledges research support from the U.S. Department of Energy, Office of Energy Efficiency and Renewable Energy, Fuel Cell Technologies Office, under Contract No. DE-AC36-08GO28308. We also thank Dr K. R. Meihaus for providing editorial assistance.

## Notes and references

- (a) N. L. Rosi, J. Eckert, M. Eddaoudi, D. T. Vodak, J. Kim, M. O'Keeffe and O. M. Yaghi, *Science*, 2003, **300**, 1127; (b) J. L. C. Rowsell and O. M. Yaghi, *Angew. Chem., Int. Ed.*, 2005, **44**, 4670; (c) M. Dincă, A. Dailly, Y. Liu, C. M. Brown, D. A. Neumann and J. R. Long, *J. Am. Chem. Soc.*, 2006, **128**, 16876; (d) D. J. Collins and H.-C. Zhou, *J. Mater. Chem.*, 2007, **17**, 3154; (e) L. J. Murray, M. Dincă and J. R. Long, *Chem. Soc. Rev.*, 2009, **38**, 1294; (f) Z. Li, G. Zhu, G. Lu, S. Qiu and X. Yao, *J. Am. Chem. Soc.*, 2010, **132**, 1490; (g) M. P. Suh, H. J. Park, T. K. Prasad and D.-W. Lim, *Chem. Rev.*, 2012, **112**, 782.
- (a) H. Wu, W. Zhou and T. Yildirim, *J. Am. Chem. Soc.*, 2009, **131**, 4995; (b) Z. Guo, H. Wu, G. Srinivas, Y. Zhou, S. Xiang, Z. Chen, Y. Yang, W. Zhou, M. O'Keeffe and B. Chen, *Angew. Chem., Int. Ed.*, 2011, **50**, 3178; (c) T. A. Makal, J.-R. Li, W. Lu and H.-C. Zhou, *Chem. Soc. Rev.*, 2012, **41**, 7761; (d) Y. Peng, V. Krungleviciute, I. Eryazici, J. T. Hupp, O. K. Farha and T. Yildirim, *J. Am. Chem. Soc.*, 2013, **135**, 11887; (e) J. A. Mason, M. Veenstra and J. R. Long, *Chem. Sci.*, 2014, **5**, 32; (f) Y. He, W. Zhou, G. Qian and B. Chen, *Chem. Soc. Rev.*, 2014, **43**, 5657.
- (a) D. Tanaka, M. Higuchi, S. Horike, R. Matsuda, Y. Kinoshita, N. Yanai and S. Kitagawa, *Chem. – Asian J.*, 2008, **3**, 1343; (b) J.-R. Li, R. J. Kuppler and H.-C. Zhou, *Chem. Soc. Rev.*, 2009, **38**, 1477; (c) J. B. DeCoste, M. H. Weston, P. E. Fuller, T. M. Tovar, G. W. Peterson, M. D. LeVan and O. K. Farha, *Angew. Chem., Int. Ed.*, 2014, **53**, 14092; (d) J. Liu, D. M. Strachan and P. K. Thallapally, *Chem. Commun.*, 2014, **50**, 466; (e) E. D. Bloch, W. L. Queen, S. Chavan,

- P. S. Wheatley, J. M. Zadrozny, R. Morris, C. M. Brown, C. Lamberti, S. Bordiga and J. R. Long, *J. Am. Chem. Soc.*, 2015, **137**, 3466.
- 4 U.S. Department of Energy, Office of Energy Efficiency & Renewable Energy, Technical System Targets: Onboard Hydrogen Storage for Light-Duty Fuel Cell Vehicles, [http://energy.gov/sites/prod/files/2015/01/f19/fcto\\_myredd\\_table\\_onboard\\_h2\\_storage\\_systems\\_doe\\_targets\\_ldv.pdf](http://energy.gov/sites/prod/files/2015/01/f19/fcto_myredd_table_onboard_h2_storage_systems_doe_targets_ldv.pdf).
- 5 E. Tsivion, J. R. Long and M. Head-Gordon, *J. Am. Chem. Soc.*, 2014, **136**, 17827.
- 6 (a) S. S.-Y. Chui, S. M.-F. Lo, J. P.-H. Charmant, A. G. Orpen and I. D. Williams, *Science*, 1999, **283**, 1148; (b) M. Dincă and J. R. Long, *Angew. Chem., Int. Ed.*, 2008, **47**, 6766; (c) P. D. C. Dietzel, R. E. Johnsen, R. Blom and H. Fjellvåg, *Chem. – Eur. J.*, 2008, **14**, 2389; (d) K. Sumida, C. M. Brown, Z. R. Herm, S. Chavan, S. Bordiga and J. R. Long, *Chem. Commun.*, 2011, **47**, 1157; (e) P. Chowdhury, S. Mekala, F. Dreisbach and S. Gumma, *Microporous Mesoporous Mater.*, 2012, **152**, 246; (f) K. Sumida, D. Stück, L. Míno, J.-D. Chai, E. D. Bloch, O. Zavorotynska, L. J. Murray, M. Dincă, S. Chavan, S. Bordiga, M. Head-Gordon and J. R. Long, *J. Am. Chem. Soc.*, 2013, **135**, 1083; (g) M. T. Kapelewski, S. J. Geier, M. R. Hudson, D. Stück, J. A. Mason, J. N. Nelson, D. J. Xiao, Z. Hulvey, E. Gilmour, S. A. FitzGerald, M. Head-Gordon, C. M. Brown and J. R. Long, *J. Am. Chem. Soc.*, 2014, **136**, 12119; (h) D. Gygi, E. D. Bloch, J. A. Mason, M. R. Hudson, M. I. Gonzalez, R. L. Siegelman, T. A. Darwish, W. L. Queen, C. M. Brown and J. R. Long, *Chem. Mater.*, 2016, **28**, 1128.
- 7 (a) K. Lee, W. C. Isley, A. Dzubak, P. Verma, S. J. Stoneburner, E. D. Bloch, D. A. Reed, M. R. Hudson, L.-C. Lin, J. Kim, C. M. Brown, J. R. Long, J. Neaton, B. Smit, C. J. Cramer, D. G. Truhlar and L. Gagliardi, *J. Am. Chem. Soc.*, 2014, **136**, 698; (b) W. L. Queen, M. R. Hudson, E. D. Bloch, J. A. Mason, M. I. Gonzalez, J. S. Lee, D. Gygi, J. D. Howe, K. Lee, T. A. Darwish, M. James, V. K. Peterson, S. J. Teat, B. Smit, J. B. Neaton, J. R. Long and C. M. Brown, *Chem. Sci.*, 2014, **5**, 4569; (c) Z. Hulvey, B. Vlasisavljevich, J. A. Mason, E. Tsivion, T. P. Dougherty, E. D. Bloch, M. Head-Gordon, D. Smit, J. R. Long and C. M. Brown, *J. Am. Chem. Soc.*, 2015, **137**, 10816.
- 8 L. Sun, T. Miyakai, S. Seki and M. Dincă, *J. Am. Chem. Soc.*, 2013, **135**, 8185.